Projection operators in multiconfiguration Dirac-Fock calculations: Application to the ground state of heliumlike ions

P. Indelicato
Laboratoire de Physique Atomique et Nucléaire, Case 93, Unité de Recherche Associée au CNRS no. 771, Université Pierre et Marie Curie, 4 place Jussieu, F-75252 Paris CEDEX 05, France
(Received 6 May 1994; revised manuscript received 14 September 1994)

The necessity of using projection operators to avoid mixing of positive and negative energy Dirac eigenstates in multiconfiguration Dirac-Fock calculations is discussed. It is shown that convergence problems observed at high Z or when the magnetic interaction was introduced in the self-consistent field (SCF) process are completely due to the absence of such projection operators in previous calculations. It is found that the presence of negative energy states prevented the diagonal Lagrange parameters (orbital energies) of correlation orbitals from approaching $-\infty$ when their weights became very small, thus causing the SCF process to fail without projection operators. A method for implementing these projection operators in Dirac-Fock programs is described. A detailed study of the effect of the introduction of projection operators, and of the self-consistent magnetic interaction in the ground state of heliumlike ions is reported. The relative importance of higher-order effects and second-order quantum electrodynamics effects is discussed.

PACS number(s): 31.30.Jv, 12.20.Ds

INTRODUCTION

Difficulties due to the existence of negative energy continua in the solution of relativistic many-electron problems have been identified very early in the history of relativistic calculations in atoms [1]. But it was only in the early 1980s that solutions derived from quantum electrodynamics (QED) were proposed by Mittleman [2] and Sucher [3,4]. However, the works both by Mittleman and by Sucher were done in the independent-particle approximation and as such were not applicable to the only relativistic many-body method available at that time, the multiconfiguration Dirac-Fock method (MCDF) [5,6]. Many-body calculations with proper treatment of the negative energy continua became possible a few years later, with the development of the relativistic many-body perturbation theory (RMBPT) [7–14]. Broyles [15] proposed a multielectron Hamiltonian based on the Feynman propagator and on the Bethe-Salpeter equation and discussed continuum dissolution in his formalism [16]. I am not aware of any practical calculation following his work.

The starting point of the MCDF approximation is the no-pair relativistic Hamiltonian. The Hamiltonian approach is not a natural one for a many-body relativistic problem because first, this problem is a multitime problem, and second, the possibility of electron-positron pair creation, always present in a relativistic framework, cannot be included in a Hamiltonian formalism. The no-pair relativistic Hamiltonian is thus at best an effective Hamiltonian, where multitime (the retardation interaction) and some pair-creation processes (vacuum polarization) are included through effective interactions (the Breit interaction) and potentials (the Uehling potential).

There has been some controversy over the necessity of using projection operators in Dirac-Fock calculations based on the no-pair Hamiltonian. Sucher [3,4,17] has been advocating the use of plane-wave projectors. It has been pointed out [12] that since negative energy continua are different for different potentials, using plane-wave or hydrogenic wave functions could introduce some unwanted negative continuum states from the "real" potential, so that the approximate answer at the no-pair level would be projection operator dependent. Such a dependency would disappear only if an exact solution of the problem is obtained. Mittleman [2] has shown that starting from a Hamiltonian including projection operators and looking for projection operators that make the energy stationary, one would get exactly Dirac-Fock projection operators, for single determinant Dirac-Fock wave functions. Grant and Quiney [18] claim to have shown (by a direct derivation from QED in Furry's bound picture) that the normalization condition on the individual wave functions in a Dirac-Fock calculation was alone able to ensure that no negative continuum states would contribute.

The latter approach, combined with Mittleman's result, was easily accepted because it provided a plausible explanation of the success of the Dirac-Fock method in the calculation of atomic energies. However, since all those derivations are done in an independent-particle approximation, none proposes a valid prescription for the multiconfiguration case. As noted in Refs. [18–20], MCDF calculations are prone to severe convergence problems when dealing with multiconfiguration cases. Up to now those failures had been attributed to "numerical" problems.

In a preliminary paper [21], where the formalism was limited to the case with only one orbital of a given symmetry, it was reported that these convergence problems are due to the influence of the negative continuum on correlation orbitals and that projection operators, although usually not needed in single-configuration Dirac-Fock calculations, are *mandatory* in the case of MCDF calculations. In the present paper, I offer a complete account of

 ©1995 The American Physical Society

a general method, applicable to any MCDF calculation. I will show some results in two-electron ions as an illustration. I would like to emphasize already that errors on the energy, associated with the omission of projection operators, are negligible for single-configuration calculations and occupied orbitals in MCDF calculations and thus most available DF calculations are still very useful.

In Sec. I, I will recall the basics of the MCDF approximation and describe a method for solving MCDF integro-differential equations. In Sec. II, I will show that the absence of projection operators leads to an inconsistency in MCDF calculations and I will propose a practical method to introduce them. In Sec. III, the effects of the inclusion of projection operators on the correlation energy of the ground state of heliumlike ions will be discussed. I will show how this modification of the MCDF method enables one to calculate corrections of higher order than what was possible before.

I. SOLUTION OF THE INHOMOGENEOUS DIRAC-FOCK EQUATION ON A COMPLETE FINITE BASIS SET

A. Fundamental equations of MCDF theory

The MCDF method is designed to provide approximate solutions to the relativistic many-body problem, beyond the one-particle approximation. It was introduced as a direct generalization of the Hartree-Fock method. It presupposes the existence of a proper, no-pair many-body Hamiltonian. Initially such a Hamiltonian was built as a direct analog of the nonrelativistic Hamiltonian. As described in the Introduction, no such equation has been derived directly from QED. For the time being I will thus use the traditional formulation of the method and use as a Hamiltonian

$$\mathcal{H}^{\rm trad} = \sum_{i=1}^{m} \mathcal{H}_D(r_i) + \sum_{i<j} \mathcal{V}\left(|\mathbf{r}_i - \mathbf{r}_j|\right), \tag{1}$$

where $\mathcal{H}_D$ is a one-electron Dirac operator and $\mathcal{V}$ is an operator representing the electron-electron interaction in some suitable form (Coulomb or Gaunt interaction for example), without any provisions for projection operators. The following will not depend on the particular choice of $\mathcal{V}$.

The atomic wave function is obtained by solving

$$\mathcal{H}^{\rm trad}\Psi_{\Pi,J,M}\left(r_1,\ldots,r_m\right) = E_{\Pi,J,M}\Psi_{\Pi,J,M}\left(r_1,\ldots,r_m\right), \tag{2}$$

where Π is the parity, J is the total angular momentum eigenvalue, and M is the eigenvalue of its projection on the z axis J_z. The MCDF method is defined by the particular choice of a trial function to solve Eq. (2) as a linear combination of configuration state functions (CSF's):

$$|\,\Psi_{\Pi,J,M}\rangle = \sum_{\nu=1}^{n} c_\nu\,|\,\nu\Pi JM\rangle. \tag{3}$$

The CSF's also are eigenfunctions of the parity Π, the total angular momentum $\mathbf{J}^2$, and its projection J_z. The label ν stands for all other values used to define unambiguously the CSF's. The CSF's, as antisymmetric products of one-electron wave functions, are expressed as

$$|\,\nu\Pi JM\rangle = \sum_{i=1}^{N_\nu} d_i \begin{vmatrix} \psi_1^i(r_1) & \cdots & \psi_m^i(r_1) \\ \vdots & \ddots & \vdots \\ \psi_1^i(r_m) & \cdots & \psi_m^i(r_m) \end{vmatrix}, \tag{4}$$

i.e., as linear combinations of Slater determinants of Dirac four-spinors. Each Dirac four-spinor is written as

$$\psi_i(r) = \frac{1}{r}\begin{pmatrix} P_i(r)\chi_{\kappa_i}^{\mu_i}(\Omega) \\ iQ_i(r)\chi_{-\kappa_i}^{\mu_i}(\Omega) \end{pmatrix}, \tag{5}$$

where $\chi_\kappa^\mu(\Omega)$ is a two-dimensional vector harmonic. It has the property that $K\psi_i(r) = \kappa\psi_i(r)$, where $K = \beta\left(\boldsymbol{\sigma}\cdot\mathbf{L}+1\right)$. The d_i are obtained by requiring that the CSF's are eigenstates of $\mathbf{J}^2$ and J_z. Writing

$$E_{\Pi,J,M} = \frac{\langle\Psi_{\Pi,J,M}\left|\mathcal{H}^{\rm trad}\right|\Psi_{\Pi,J,M}\rangle}{\langle\Psi_{\Pi,J,M}|\Psi_{\Pi,J,M}\rangle} \tag{6}$$

and using a variational principle on the coefficients c_ν and on the large and small radial components of the wave function $P_i(r)$ and $Q_i(r)$, one obtains the fundamental equations of the MCDF method. Writing $\partial E_{\Pi,J,M}/\partial c_\nu = 0$ leads to a Hamiltonian matrix from which the c_ν are determined by diagonalization. Variation with respect to the radial wave functions [formally written as $\partial E_{\Pi,J,M}/\partial f_i(r) = 0$, with f being either P or Q] leads to a set of coupled integro-differential equations

$$\begin{pmatrix} V_{\rm DF}^i(r) & -\frac{d}{dr}+\frac{\kappa_i}{r} \\ \frac{d}{dr}+\frac{\kappa_i}{r} & V_{\rm DF}^i(r)-2mc \end{pmatrix}\begin{pmatrix} P_i(r) \\ Q_i(r) \end{pmatrix}$$

$$= \alpha\lambda_{i,i}\begin{pmatrix} P_i(r) \\ Q_i(r) \end{pmatrix} + \begin{pmatrix} X_P^i(r) \\ X_Q^i(r) \end{pmatrix} + \sum_{j\neq i}\lambda_{j,i}\begin{pmatrix} P_j(r) \\ Q_j(r) \end{pmatrix}, \tag{7}$$

where $V_{\rm DF}^i(r)$ is the sum of the direct Dirac-Fock potential and the nuclear potential, $(X_P^i(r), X_Q^i(r))$ are the exchange potentials for the large and small components, respectively, $\lambda_{i,i}$ is the diagonal Lagrange parameter used to enforce normalization, and $\lambda_{i,j}$ are off-diagonal Lagrange parameters used to enforce orthogonality constraints between orbitals of the same κ:

$$\int_0^\infty dr\left[P_i(r)P_j(r)+Q_i(r)Q_j(r)\right] = \delta\left(\kappa_i,\kappa_j\right)\delta\left(n_i,n_j\right). \tag{8}$$

B. Solution of the MCDF equation using a finite basis set

The set of coupled integro-differential equations (7) of Sec. I A is solved by a self-consistent field process (SCF). A set of initial wave functions is chosen. Then the coefficients c_ν are determined by diagonalization of

the Hamiltonian matrix. Direct and exchange Dirac-Fock potentials for a given orbital are calculated and Eq. (7) is solved. Such a cycle is repeated for each wave function until all wave functions are stable to a given accuracy (usually 1 part in 10^5 or better), while diagonal Lagrange parameters are required to be stable to 5×10^{-7}. Diagonalization and self-consistent cycles are repeated until complete self-consistency is obtained.

Individual integro-differential equations (7) are often solved by finite-difference or predictor-corrector methods, with some combined dichotomy–Newton-Raphson algorithm to get the eigenvalue $\lambda_{n,n}$. The wave function must be regular at the origin and infinity and it must be continuous. However, it is very often difficult to achieve convergence for orbitals with very small effective occupations (the effective occupation of an orbital is defined as the product of the number of electrons in the orbital and c_ν^2, orbitals with small effective occupations are called correlation orbitals). In that case the exchange potentials are large and Eq. (7) has a solution very different from the solution of the corresponding homogeneous equation, obtained by setting exchange potentials and off-diagonal Lagrange parameters to zero.

It is now widely accepted that one can use the Breit operator beyond first-order perturbation theory, provided projection operators are used. Thus it should be possible to include the magnetic interaction in the definition of direct and exchange potentials to get magnetic correlation effects. Also, since it is a small perturbation to the Coulomb interaction, one would expect that it will not change the difficulty of the calculation beyond the necessary angular momentum algebra involved. However, the magnetic interaction term was found to increase convergence difficulties by orders of magnitude. This is because the magnetic interaction adds a large contribution to the exchange potentials, causing most algorithms used to solve Eq. (7) to fail.

In the rest of this section I will describe a general method to solve Eq. (7) or any equation with the same structure. The idea is to use a *complete* set of solutions of the associated homogeneous equation. In order to simplify the notation and to get a practical method I will suppose at this stage that the atom is enclosed in a finite box with a radius large enough to get a good approximation, with some suitable set of boundary conditions. In that case one obtains a finite set, with the continuum described by discrete functions. This is of no fundamental importance; it is just done as a matter of practical convenience.

Let us denote by $\{\phi_n^i(r), i = 1, ..., 2N\}$ such a set of solutions where n is the level number and i the position of the solution in the set. For each n the set $\{\phi_n^i(r), i = 1, ..., 2N\}$ is complete. Each $\phi_n^i(r)$ obeys

$$\begin{pmatrix} V_{\rm DF}^n(r) & -\frac{d}{dr} + \frac{\kappa_n}{r} \\ \frac{d}{dr} + \frac{\kappa_n}{r} & V_{\rm DF}^n(r) - 2mc \end{pmatrix} \phi_n^i(r) = \alpha \epsilon_n^i \phi_n^i(r). \quad (9)$$

It is very important to remember that in the relativistic case, a complete set spans both positive and negative energy solutions. Solutions $i = 1, ..., N$ represent the continuum $\epsilon_n^i < -2mc^2$ and solutions $i = N+1, \ldots, 2N$ represent bound states (the few first ones) and the $\epsilon_n^i > 0$ continuum using the conventions of Eq. (9).

Since the ϕ_n^i form a complete set, the solution of Eq. (7) can be expanded as a linear combination of basis set wave functions and the exchange potentials read

$$\begin{pmatrix} P_n(r) \\ Q_n(r) \end{pmatrix} = \sum_i s_i \phi_n^i, \quad (10)$$

$$\begin{pmatrix} X_P^n(r) \\ X_Q^n(r) \end{pmatrix} = \sum_i x_i \phi_n^i. \quad (11)$$

From Eqs. (7) and (9)–(11) and the orthonormality condition of the basis set, one gets

$$s_l^n = \frac{x_l^n + \sum_{i \neq n} \lambda_{i,n} s_l^i}{\alpha (\epsilon_n^l - \lambda_{n,n})}. \quad (12)$$

It is important to notice that if s_l^n are unknowns to be determined in the calculation, s_l^i, $i \neq n$, are results of previous iterations and are fixed parameters. The x_l^n also depend on the solutions from previous iterations.

From the normalization condition of Eq. (8) the norm of $\psi_n(r)$ can be written as:

$$\begin{aligned} N(\lambda_{n,n}) &= \sum_l \left(s_n^l\right)^2 \\ &= \sum_l \left(\frac{x_l^n + \sum_{i \neq n} \lambda_{i,n} s_l^i}{\alpha (\epsilon_n^l - \lambda_{n,n})} \right)^2 . \end{aligned} \quad (13)$$

Solving for $N(\lambda_{n,n}) = 1$ will enable one to get the solution of Eq. (7) provided that the off-diagonal Lagrange parameters are known.

C. Evaluation of the off-diagonal Lagrange parameters

Equation (8) for $i \neq n$ provides a system of equations which can be solved to give all needed off-diagonal Lagrange parameters. The orthogonality relations from Eq. (8) reduce to

$$\begin{aligned} 0 &= \sum_l s_l^n s_l^i \\ &= \sum_l \frac{x_l^n s_l^i + \sum_{j \neq n} \lambda_{j,n} s_l^j s_l^i}{\alpha (\epsilon_n^l - \lambda_{n,n})}. \end{aligned} \quad (14)$$

This is a set of linear equations which can be recast as

$$\sum_{j \neq n} \lambda_{j,n} \left(\sum_l \frac{s_l^i s_l^j}{\epsilon_n^l - \lambda_{n,n}} \right) = - \left(\sum_l \frac{x_l^n s_l^i}{(\epsilon_n^l - \lambda_{n,n})} \right), \quad (15)$$

if $N_{\rm ort}$ is the number of orbitals, different from ψ_n with identical symmetry (which have thus to be kept orthogonal to one another). Equation (15) leads to a matrix equation

$$\begin{pmatrix} \left(\sum_l \frac{s_l^{n_1} s_l^{n_1}}{\epsilon_n^l - \lambda_{n,n}}\right) & \left(\sum_l \frac{s_l^{n_1} s_l^{n_2}}{\epsilon_n^l - \lambda_{n,n}}\right) & \cdots & \left(\sum_l \frac{s_l^{n_1} s_l^{n_{N_{\rm ort}}}}{\epsilon_n^l - \lambda_{n,n}}\right) \\ \left(\sum_l \frac{s_l^{n_2} s_l^{n_1}}{\epsilon_n^l - \lambda_{n,n}}\right) & \cdots & \cdots & \left(\sum_l \frac{s_l^{n_2} s_l^{n_{N_{\rm ort}}}}{\epsilon_n^l - \lambda_{n,n}}\right) \\ \vdots & \vdots & \ddots & \vdots \\ \left(\sum_l \frac{s_l^{n_{N_{\rm ort}}} s_l^{n_1}}{\epsilon_n^l - \lambda_{n,n}}\right) & \cdots & \cdots & \left(\sum_l \frac{s_l^{n_{N_{\rm ort}}} s_l^{n_{N_{\rm ort}}}}{\epsilon_n^l - \lambda_{n,n}}\right) \end{pmatrix} \begin{pmatrix} \lambda_{n_1,n} \\ \lambda_{n_2,n} \\ \vdots \\ \lambda_{n_{N_{\rm ort}},n} \end{pmatrix} = - \begin{pmatrix} \sum_l \frac{x_l^n s_l^{n_1}}{(\epsilon_n^l - \lambda_{n,n})} \\ \sum_l \frac{x_l^n s_l^{n_2}}{(\epsilon_n^l - \lambda_{n,n})} \\ \vdots \\ \sum_l \frac{x_l^n s_l^{n_{N_{\rm ort}}}}{(\epsilon_n^l - \lambda_{n,n})} \end{pmatrix} . \quad (16)$$

This equation is easily solved for the off-diagonal Lagrange parameters by usual matrix inversion techniques. One is now faced with the simultaneous solution of Eqs. (13) and (16) for both $\lambda_{n,n}$ and the off-diagonal Lagrange parameters. This is done by combining standard dichotomy and Newton-Raphson techniques (see, for example, [22]). At this stage it is useful to note that the method just described is general and could be used in nonrelativistic Hartree-Fock calculations as well.

D. Structure of the solution of the inhomogeneous Dirac-Fock equation

In Secs. IB and IC, I have described the basic formalism for the solution of the inhomogeneous Dirac-Fock equation on a basis set. But because it is possible to use a finite basis set by enclosing the atom in a box, very important physical information can be deduced from the structure of the solutions of this inhomogeneous Dirac-Fock equation. In particular, one can easily highlight the essential role of the negative energy continuum $\lambda_{n,n} \leq -2mc^2$.

The study of the solution is best done by comparing two different examples. In order to simplify the figures, I have chosen two cases of orbitals for which no other orbital of the same symmetry is present. In that case only Eq. (13) needs to be solved since no off-diagonal Lagrange parameter is needed. In Fig. 1 the evolution of the norm of $\psi_n(r)$ has been plotted as a function of the diagonal Lagrange parameter for the $2p_{1/2}$ orbital and $Z = 100$. The configuration set consists of $1s^2$, $2s^2$, $2p_{1/2}^2$, and $2p_{3/2}^2$. The norm has a pole of order 2 for the energy of each solution of the homogeneous equation. This fact has been reported long ago by Griffin *et al.* for the Hartree-Fock case [23]. Since a discrete basis set has been chosen, there are also poles in the $\lambda_{n,n} > 0$ and $\lambda_{n,n} < -2mc^2$ "continua." If a continuous basis set had been used, there would have been two branch cuts for these continua. Since the vertical scale of the figure is very large compared to 1, there is only one solution to Eq. (13) and it corresponds to a diagonal Lagrange parameter $\lambda_{n,n} \approx -17672$ a.u.

In Fig. 2 a very different case is represented. It is the plot of the norm of a $5g_{7/2}$ orbital in a calculation involving a configuration set composed of $1s^2$, $2s^2$, $2p_{1/2}^2$, $2p_{3/2}^2$,...,$5g_{7/2}^2$, and $5g_{9/2}^2$, again at $Z = 100$. At first glance one can see that there are no solutions of norm 1 in this case. The exchange potential for the $5g_{7/2}$ orbital at $Z = 100$ is so large that no solution can be found for any $\lambda_{n,n} < 0$. The presence of the negative continuum prevents the norm to become lower than 1 because there are poles all along the axis for $\lambda_{n,n} < -2mc^2$. This contrasts with the Hartree-Fock case: because there is no pole below the lowest bound state of the homogeneous equation, $N(\lambda_{n,n}) \to 0$ when $\lambda_{n,n} \to -\infty$ and thus there is always a solution, although it will be very negative if the exchange coefficients are very large.

These two examples show very clearly the two different possible cases when dealing with $\mathcal{H}^{\rm trad}$. If the mixing coefficients c_ν are large (i.e., at low Z and/or small n), there are solutions for the inhomogeneous Dirac-Fock equation. If the mixing coefficients are small (i.e., at high Z and/or large n), the solution may not exist *because of the* $\lambda_{n,n} < -2mc^2$ *continuum.*

As mentioned when discussing Eq. (9), the equation that is solved at a given iteration depends on results from all wave functions at earlier iterations. So one has to be sure that this is not a local condition due to a poor choice of initial wave functions. In order to avoid such a problem, all results presented here have been done in an incremental way. New configurations are added one

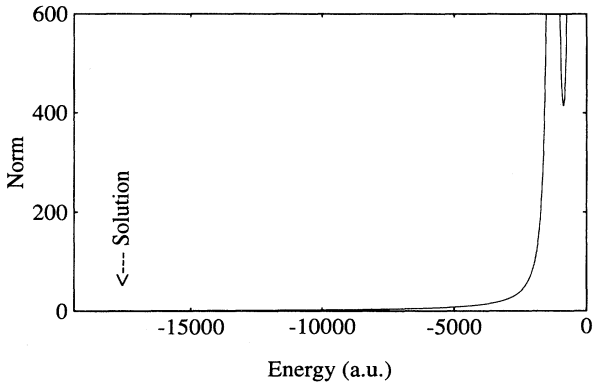

FIG. 1. Norm of the solution of the inhomogeneous differential equation (7), ψ_n, as a function of the energy. The configurations used are $1s^2$, $2s^2$, $2p_{1/2}^2$, and $2p_{3/2}^2$. The wave function presented is $2p_{1/2}$ for $Z = 100$. Only the region where bound solutions are present is plotted. Note that the solution of $N(E) = 1$ can be met only at $E \approx -17\,672$ a.u. $> -2mc^2 = -37\,557$ a.u. and that the vertical scale reaches 600.

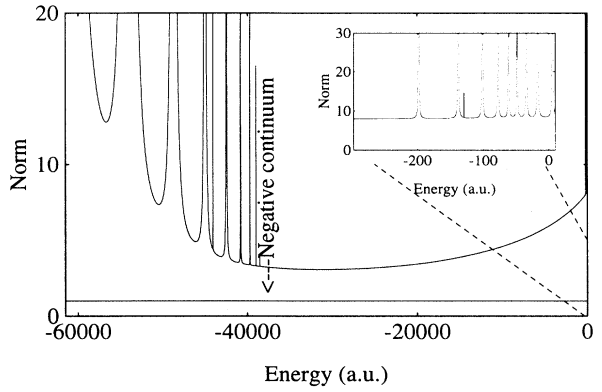

FIG. 2. Norm of the solution of the inhomogeneous differential equation (7), ψ_n, as a function of the energy. The configurations used are $1s^2$, $2s^2$, $2p_{1/2}^2$, and $2p_{3/2}^2$,..., $5g_{7/2}^2$, $5g_{9/2}^2$. The wave function presented is $5g_{7/2}$ for $Z = 100$. The inset represents the homogeneous equation's bound-state area, which is indistinguishable from the vertical axis at this scale.

by one and full self-consistency is achieved at each stage. So only the last orbital that is being added can be very different from its converged form. More checks for this problem have been done and will be reported below.

When off-diagonal Lagrange multipliers are present, there are no longer poles at the solutions of the homogeneous equations but only maxima. The same conclusions hold, however, because when exchange potentials are large the maxima are large compared to 1. The disappearance of the poles can be easily deduced from Eq. (16), in a case with only one Lagrange parameter. Then, close to ϵ_0, $\lambda_{n_1,n} \approx -x_0^n/(s_0^{n_1})$ and the numerator $x_0^n + \lambda_{n_1,n} s_0^{n_1}$ cancels as $E \to \epsilon_0$. A more complete calculation shows that $N(\lambda_{n,n})$ is finite and has a maximum for $\lambda_{n,n} \to \epsilon_0$.

II. PROJECTION OPERATORS IN MCDF THEORY

A. Demonstration of the necessity of using projection operators in MCDF calculation

The results of Sec. I D show the importance of the role of the negative energy continuum in the existence of a solution to the inhomogeneous Dirac-Fock equation. In this section I will show the relationship between this continuum and the convergence of the self-consistent field process.

Once the method of solution described in the preceding section was implemented, it was tested on the ground state of heliumlike ions. With the finite-difference method that has been used up to now, it was possible to achieve convergence with a set of configurations composed at most of $1s^2$, $2s^2$, ..., $4d^2$, $4f^2$. This was obtainable with great difficulties (a lot of tuning of initial wave functions and mixing coefficients) and only for atomic numbers ranging from 10 to 66. In all these calculations the aim is always to reach full self-consistency, i.e., no orbital or mixing coefficient is kept frozen in any way. Whatever was tried would not make the $4f^2$ configuration converge for $Z = 67$. By the time uranium ($Z = 92$) was reached, it was impossible to get any convergence past $4s^2$. The new method, in contrast, is very efficient, with almost no tuning of initial wave functions and mixing coefficients. I have been able to reach convergence for a basis set as large as $1s^2$, $2s^2$, ..., $4d^2$, $4f^2$, $5s^2$,..., $5f^2$, $5g^2$, at low Z. The power of the method, which always finds the orbital energy and which keeps all orbitals of identical symmetry perfectly orthogonal at each stage of the calculation, is then demonstrated. The method works very well also if one takes the speed of light $c = 1/\alpha$ to infinity for any atomic number (this amounts to a multiconfiguration Hartree-Fock calculation). However, the MCDF calculation still fails when the atomic number increases. There are no normalized $5g$ orbitals to be found above $Z = 54$ and no normalized $4f$ at $Z = 67$, exactly as in finite-differences methods.

However, the reason for this lack of convergence is now obvious from the discussion of Sec. I D: Eq. (13) has no solution, i.e., $N(\lambda_{n,n})$ is always larger than 1 because of the presence of the negative energy continuum. The finite-difference method failed for the same reason, except that it would not give any insight into why it has been failing.

The fact that $\lambda_{i,i}$ has to go to $-\infty$ for large principal quantum number correlation orbitals can easily be derived from very simple physical arguments. Correlation orbitals must be localized in the same area as the occupied orbitals. Their radii must then be of comparable size. To contribute to the correlation energy of the ground state of a two-electron system, the ith correlation orbital of principal quantum number n_i must have a radius r_i comparable to r_{1s}. Each correlation orbital is described by an effective atomic number $Z_{i,\text{eff}}$. Thus $r_i = n_i^2 a_0 / Z_{i,\text{eff}}$ (a_0 is the Bohr radius). Orbital $1s$ radius is $r_{1s} = a_0/Z$. From that one deduces that $Z_{i,\text{eff}} \approx n_i^2 Z$, using $r_{1s} \approx r_i$. Thus the diagonal Lagrange parameter is $\lambda_{i,i} = -Z_{i,\text{eff}}^2/2n_i^2 = -n_i^2 Z^2/2$. This very simple argument shows that when the principal quantum number of a correlation orbital goes to infinity, the diagonal Lagrange parameter of the orbital must go to $-\infty$. This is always possible in the nonrelativistic case, but *this cannot happen in the Dirac-Fock case because of the existence of the negative energy continuum.*

Two options are now possible. Either one has to admit that in the MCDF case, the size of the configuration set that may be used is finite and changes with the atomic number, while it can be infinite in the nonrelativistic case, or one must introduce a projection operator that will remove the negative energy continuum and allow $\lambda_{n,n}$ to become as negative as needed. The first method introduces a very unappealing dissymmetry between the nonrelativistic and the relativistic case. Moreover, it makes it impossible to introduce the magnetic interaction in the self-consistent field (SCF) because this interaction increases the exchange potential, which leads to even more negative diagonal Lagrange multipliers. This is not at all satisfactory, and the only reason-

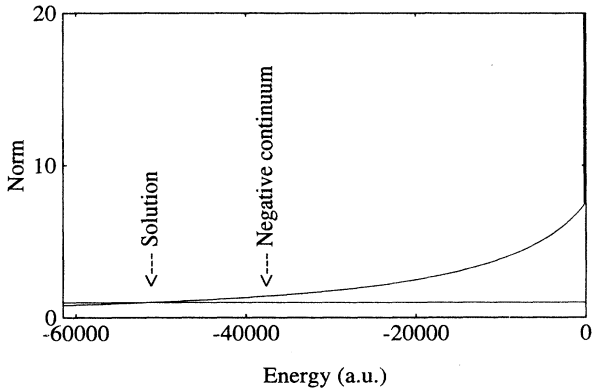

FIG. 3. Norm of the solution of the inhomogeneous differential equation (7), ψ_n, as a function of the energy in the same case as in Fig. 2, but the projection has now been performed, removing the negative energy continuum. The solution is now at $-51\,364$ a.u. $< -2mc^2$.

able solution, which is consistent with results obtained in RMBPT calculations, is to introduce proper projection operators.

The effect of projecting out the negative energy continuum can be seen in Fig. 3, which deals with the same case as Fig. 2. The projection is accomplished simply by excluding all negative energy continuum states from the summation in the definition of the norm in Eq. (13) and from the definition of the solution of the inhomogeneous Dirac-Fock equation (7). There are then no more obstacles to prevent $\lambda_{n,n}$ from becoming smaller than $-2mc^2$ and the real solution is found there, as can be seen from Fig. 3. One obtains $\lambda_{n,n} \approx -51\,364$ a.u. $< -2mc^2 = -37\,557.7$ a.u. The magnetic interaction has been used in defining the potentials and still a solution is easily found, although it is a very high Z.

Obviously this way of showing the necessity of using projection operators does not stem directly from QED. Up to now nobody seems to have been able to do that beyond the independent-particles approximation. One can use, however, the obvious solution described above, which is suggested by the finite basis set method itself and was used in all RMBPT calculations. All summations are thus limited to basis functions of energy larger than $-2mc^2$. The downside of this empirical approach is that the choice of projection operator is not unique because the definition of the homogeneous equation is not. For example, some terms in Eq. (7) can be shifted from the exchange potential to the Dirac-Fock potential. This leads to a different basis set, but should leave the solution unchanged if the method is to have some applications. I have checked that the final results of the MCDF calculation are invariant in a limited number of transformations of the exchange potential.

B. Practical implementation of projection operators in MCDF theory

The method I have described up to now is completely general. Except for transforming some discrete sums into an integrals and sums combination, it could even be applied to a continuous basis set. In this section I describe briefly the implementation of the method in Desclaux's MCDF code [6]. For practical reasons, the set of solutions is itself expressed as a linear combination of another basis set, chosen for easy numerical implementation. There are thus two basis sets involved, a physical one composed of solutions of the homogeneous equations (9) and a numerical one.

Calculations done in the RMBPT framework have used two methods to get a finite basis set and manageable finite sums rather than integrals over continua. One of these methods is based on B splines as developed by Johnson, Blundell, and Sapirstein [8] and the other is based on a discretization of the equations as developed by Salomonson and Oster [14,24]. For the same practical reasons I have built the program on the B-spline basis set, for which integrations and projections of numerical functions are very easy to handle.

The code I used and the derivation of the solutions of Eq. (9) are thus exactly identical to those described by Johnson *et al.* It has been described in detail in Ref. [8] and will not be reproduced here.

In all the calculations presented in the following, I have used ninth-order splines and 45 collocation points. The mesh for tabulating the wave functions when using the finite-difference method had around 400 points, 41 of which were located inside the nucleus. Mesh points were located following the relation $nh = \ln[r(n)/r(1)] + ar(n)$, with $a = 0.1$ and $h = 0.03$. The distance between mesh points was thus exponentially increasing at short distances and turning progressively linear at large distances.

III. APPLICATION TO THE GROUND STATE OF HELIUMLIKE IONS

A. Effect of the projection operator on the ground-state energies of heliumlike ions

The ground state of heliumlike ions is a good test case for the formalism described above. The electron-electron interaction can be written as

$$\mathcal{V}_{ij} = \mathcal{V}_{ij}^{C} + \mathcal{V}_{ij}^{G} + \mathcal{V}_{ij}^{\mathrm{BR}} + \mathcal{V}_{ij}^{\mathrm{HOR}}, \tag{17}$$

where

$$\mathcal{V}_{ij}^{C} = \frac{1}{r_{ij}} \tag{18}$$

is the Coulomb interaction,

$$\mathcal{V}_{ij}^{G} = -\frac{\boldsymbol{\alpha}_i \cdot \boldsymbol{\alpha}_j}{r_{ij}} \tag{19}$$

is the Gaunt interaction,

$$\mathcal{V}_{ij}^{\mathrm{BR}} = \frac{\boldsymbol{\alpha}_i \cdot \boldsymbol{\alpha}_j}{2r_{ij}} - \frac{(\boldsymbol{\alpha}_i \cdot \boldsymbol{r}_{ij})\,(\boldsymbol{\alpha}_j \cdot \boldsymbol{r}_{ij})}{2r_{ij}} \tag{20}$$

is the Breit retardation, and

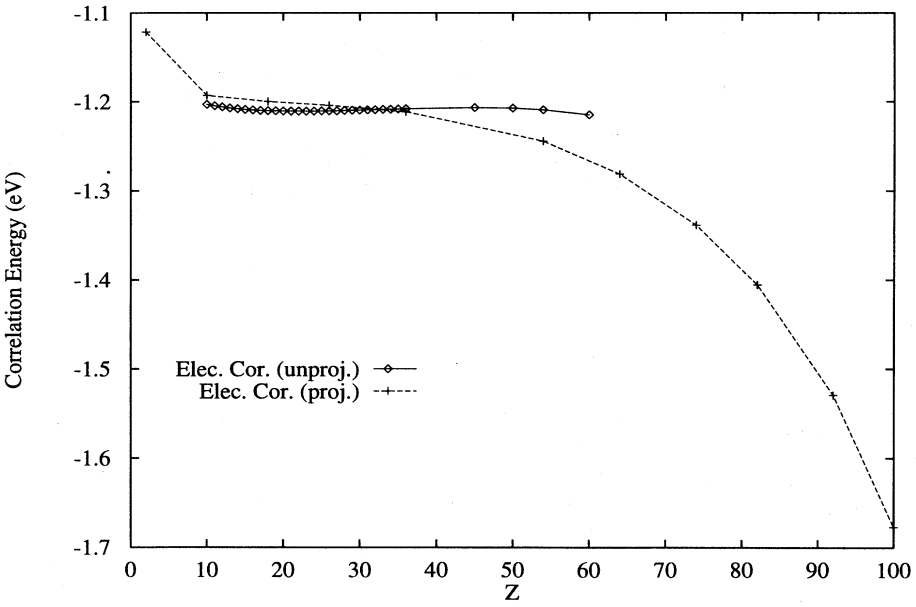

FIG. 4. Comparison of electrostatic correlation energy with [Elec. Cor. (unproj.)] and without [Elec. Cor. (proj.)] a projection operator. The configuration set is $1s^2$, $2s^2$,..., $4f^2$.

$$\mathcal{V}_{ij}^{\mathrm{HOR}} = -\frac{\boldsymbol{\alpha}_i \cdot \boldsymbol{\alpha}_j}{r_{ij}} \left[\cos\left(\omega_{ij} r_{ij}\right) - 1\right] - \left(\boldsymbol{\alpha}_i \cdot \boldsymbol{\nabla}_i\right)\left(\boldsymbol{\alpha}_j \cdot \boldsymbol{\nabla}_j\right) \frac{\cos\left(\omega_{ij} r_{ij}\right) - 1}{\omega_{ij}^2 r_{ij}} - \mathcal{V}_{ij}^{\mathrm{BR}} \tag{21}$$

represents higher-order retardation. Here $r_{ij} = |\boldsymbol{r}_i - \boldsymbol{r}_j|$ is the interelectronic distance and ω_{ij} the energy of the photon exchanged between the electrons.

In this section the Coulomb interaction $\mathcal{V}^C$ is used as the two-body operator $\mathcal{V}$ in the definition of the relativistic Hamiltonian (1). Thus only this interaction contributes to the direct and exchange potentials definition and to the definition of the projection operators. The magnetic (or Gaunt) interaction $\mathcal{V}^G$ is treated as a first-order perturbation. The total magnetic energy is thus $E^G = \langle \Psi_{\Pi,J,M} \mid \sum_{i<j} \mathcal{V}_{ij}^G \mid \Psi_{\Pi,J,M} \rangle$.

With the implementation of projection operators in the Dirac-Fock code, I have been able to achieve convergence for all Z between 2 and 100, with a CSF set extended to $5g^2$, while $Z = 66$ (for CSF sets extending up to $4f^2$) was the limit in previous calculations [19]. In Ref. [19] a standard finite difference technique was used to solve the inhomogeneous Dirac-Fock equation. In Fig. 4, I have plotted the results of both calculations. The change in the shape of the correlation energy in the vicinity of $Z = 66$, where the $4f^2$ diagonal Lagrange multiplier reaches $-2mc^2$, is pretty obvious. A small part of the difference, however, could be due to the fact

TABLE I. Comparison between projected and unprojected orbital properties for $Z = 92$, the diagonal Lagrange multipliers (a.u.). The following abbreviations are used: $4s$ only, only the $4s$ orbital is calculated with projection operators; none (FD), all orbitals calculated without projection operators (using finite-difference method); none (BS), all orbitals calculated without projection operators (using B spline method); all, all orbitals calculated with projection operators. All configurations from $1s^2$ to $4s^2$ are included (maximum set where convergence could be achieved with all methods).

Orbital	$4s$ only	None (FD)	None (BS)	All
$1s_{1/2}$	−4783.379	−4783.379	−4783.379	−4783.385
$2p_{1/2}$	−8890.197	−8890.078	−8890.017	−10767.134
$3d_{3/2}$	−9455.647	−8887.684	−9459.019	−19724.496
$3p_{1/2}$	−10409.011	−10405.833	−10405.532	−20978.298
$2s_{1/2}$	−10704.968	−10719.765	−10719.874	−11408.896
$2p_{3/2}$	−12617.515	−12617.499	−12617.519	−12970.090
$3s_{1/2}$	−14054.748	−15332.277	−15328.908	−21529.479
$3p_{3/2}$	−18977.477	−18977.680	−18977.555	−27111.285
$3d_{5/2}$	−20168.409	−20168.372	−20168.414	−23431.608
$4s_{1/2}$	−39056.529	−21007.140	−21025.981	−41307.215
total energy	−9637.378	−9637.378	−9637.378	−9637.383

TABLE II. Comparison between projected and unprojected orbital properties for $Z = 92$, the distance at which the electronic density is maximum (a.u.). Only the Coulomb interaction is included. The following abbreviations are used: $4s$ only, only the $4s$ orbital is calculated with projection operators; none, all orbitals calculated without projection operators (using finite-difference method); all, all orbitals calculated with projection operators. All configurations from $1s^2$ to $4s^2$ are included (the maximum is set where convergence could be achieved with all methods).

Orbital	$4s$ only	None	All
$1s_{1/2}$	8.114×10^{-03}	8.114×10^{-03}	8.114×10^{-03}
$2p_{1/2}$	8.374×10^{-03}	8.375×10^{-03}	1.009×10^{-02}
$3d_{3/2}$	1.205×10^{-02}	1.215×10^{-02}	1.061×10^{-02}
$3p_{1/2}$	3.675×10^{-03}	3.675×10^{-03}	4.005×10^{-03}
$2s_{1/2}$	3.771×10^{-03}	3.767×10^{-03}	3.622×10^{-03}
$2p_{3/2}$	1.216×10^{-02}	1.216×10^{-02}	1.174×10^{-02}
$3s_{1/2}$	2.712×10^{-03}	2.517×10^{-03}	2.166×10^{-03}
$3p_{3/2}$	6.246×10^{-03}	6.246×10^{-03}	5.495×10^{-03}
$3d_{5/2}$	1.241×10^{-02}	1.241×10^{-02}	1.129×10^{-02}
$4s_{1/2}$	1.444×10^{-03}	2.541×10^{-03}	1.353×10^{-03}

that the finite-difference method is more accurate (when it works) than the spline method. Another difference is due to the fact that in the new method it is not possible to enforce exactly the relationship between $\lambda_{i,j}$ and $\lambda_{j,i}$ because of the presence of the pole and the necessity to have an exact cancellation in both the numerator and the denominator in Eq. (16). In contrast, the relationship was exactly enforced in the finite-difference method. However, the difference between the two off-diagonal Lagrange multipliers is small at convergence. The results of the detailed example discussed in the following paragraphs show that this approximation has negligible effects on total energies, diagonal Lagrange parameters, and radial wave functions.

The results of different test calculations are presented and compared in Tables I–IV. Different orbital properties (the radius of maximum density and diagonal and nondiagonal Lagrange multipliers) as well as configuration mixing coefficients for heliumlike uranium are tabulated for three cases. The configuration set consists of $1s^2$,...,$4s^2$ because $4s$ was the most excited orbital that could be made to converge in uranium without projection operators. In the first column of these four tables displayed are results from a calculation where $4s$ was the only orbital calculated using projection operators. In the second column no projection operators were used and in the last column all orbitals, except for $1s$, were evaluated using projection operators. All the calculations are performed using a Fermi model for the nucleus, with a rms radius of 5.75 fm and a thickness parameter of 2.3 fm.

In Table I an extra column is devoted to an unprojected calculation of diagonal Lagrange parameters, using the finite basis set method of solution, to compare with the finite-difference method. Most numbers are very close. The value for $3d_{3/2}$, however, is different, but resembles closely the finite-difference value obtained when the $4s$ orbital alone is projected. The reasons for such a behavior are not understood.

As expected from the discussion above, the diagonal Lagrange parameter for the $4s$ orbital becomes more negative when its projection operator is included, if everything else is kept constant. In Fig. 5 the large and small radial components of $4s$ are displayed for projected and unprojected calculations. The basis set method without projector and the finite-difference method give radial functions that are virtually indistinguishable. The effect of including projection operators changes strikingly the radial wave function, which is obviously correlated with the energy change. One can also notice that orbitals with $j = l - 1/2$ are more strongly changed than those with $j = l + 1/2$, as expected for an effect of relativistic origin (a $p_{1/2}$ orbital, for example, exhibits a strong s behavior for high Z), yet the changes in the total energy (Table III) remain very small.

The electrostatic correlation energy is defined here as the difference between the total energy for the largest possible set of configurations (here $1s^2$,..., $5g^2$) and the total energy for the single-particle Dirac-Fock approximation (here $1s^2$ only). The magnetic correlation energy is defined as the difference between the total magnetic energies between the same wave functions.

In Fig. 6, I have plotted the result of a calculation including all configurations up to $5g^2$ and the exact nonrelativistic value from Ref. [25]. The effects of relativity at high Z are strong, but beyond the reach of any experiment that can be reasonably expected in the near future. Moreover, much larger effects due to uncertainty in the nuclear size, in nuclear polarization, and in uncalculated QED terms would certainly conceal it.

In contrast, the magnetic correlation energy is very large and dominates the total correlation energy for all atomic numbers above $Z = 54$. This contribution reaches

TABLE III. Comparison between projected and unprojected orbital properties for $Z = 92$, the off-diagonal Lagrange multipliers (a.u.). See Table II for definitions.

Orbitals	$4s$ only	None	All
$1s_{1/2}2s_{1/2}$	-2.969×10^{-02}	-2.966×10^{-02}	-3.045×10^{-02}
$1s_{1/2}3s_{1/2}$	1.284×10^{-04}	1.392×10^{-04}	-2.259×10^{-04}
$1s_{1/2}4s_{1/2}$	-2.195×10^{-05}	-3.070×10^{-05}	-1.221×10^{-05}
$2s_{1/2}3s_{1/2}$	$-4.355\times10^{+02}$	$-4.158\times10^{+02}$	$-6.503\times10^{+02}$
$2s_{1/2}4s_{1/2}$	$-4.255\times10^{+01}$	$1.764\times10^{+00}$	$-9.259\times10^{+00}$
$3s_{1/2}4s_{1/2}$	$-3.419\times10^{+03}$	$-1.215\times10^{+03}$	$-2.615\times10^{+03}$
$2p_{1/2}3p_{1/2}$	$1.091\times10^{+02}$	$1.090\times10^{+02}$	$6.419\times10^{+02}$
$2p_{3/2}3p_{3/2}$	$9.168\times10^{+02}$	$9.168\times10^{+02}$	$1.083\times10^{+03}$

TABLE IV. Comparison between projected and unprojected orbital properties for $Z = 92$, the configuration mixing coefficients. See Table II for definitions.

Orbital	$4s$ only	None	All
$1s^2_{1/2}$	0.999998	0.999998	0.999998
$2p^2_{1/2}$	0.000606	0.000606	0.000604
$3d^2_{3/2}$	−0.000111	−0.000105	−0.000111
$3p^2_{1/2}$	0.000112	0.000112	0.000121
$2s^2_{1/2}$	−0.001379	−0.001378	−0.001359
$2p^2_{3/2}$	0.001071	0.001071	0.001060
$3s^2_{1/2}$	−0.000240	−0.000230	−0.000223
$3p^2_{3/2}$	0.000256	0.000256	0.000232
$3d^2_{5/2}$	0.000264	0.000264	0.000251
$4s^2_{1/2}$	−0.000072	−0.000064	−0.000061

6 eV in uranium and thus should be an observable contribution in the next generation of experiments.

As a final check that convergence problems encountered with the finite-difference method were not due to poor initial wave functions, as discussed above, I tried to use the self-consistent orbitals obtained with projection operators as initial wave functions for a new calculation without a projection operator (using either the method described here or the finite-difference method). This provided very good initial wave functions for light elements, for which the negative continuum does not interfere. But calculation for large Z always failed. Moreover, the method that I just described *never* failed for nonrelativistic cases, for any set of the reasonable initial wave functions I tried. It would be surprising that such a consistent behavior would have happened only by chance.

B. Effect of self-consistent magnetic interaction on heliumlike ions ground-state energy

In the preceding subsection I described the effects of a complete relativistic treatment and of the introduction of projection operators in the electrostatic and magnetic correlation energy. As is customary for low Z or for outer-shell electron calculations, I have treated the magnetic interaction as a perturbation. There is, however, no fundamental reason to do so, and for very heavy ions, this leads to the omission of cross terms that could be important. In the past, several attempts have been made to evaluate those crossed terms, but as explained above, these attempts failed because the exchange potentials were increased by a large amount even for elements with moderate atomic numbers. With the use of the projection operators, such a problem vanishes and there is no more difference in convergence between calculations where the Coulomb interaction or the Gaunt interaction is used in the SCF. It should be noted that when one uses the Gaunt interaction in the SCF, the electrostatic and the magnetic interactions are both treated on the same footing and appear in the definition of the c_ν as well as in the definition of the direct and exchange potentials. Using the magnetic part of the interaction only in the diagonalization of the Hamiltonian, as it has been done sometimes, does not have the same impact on the final result because it only slightly changes the exchange potentials through mixing coefficients.

As an example, the single configuration ground-state energy for heliumlike uranium is −9625.22 a.u., while the final energy including all $n = 1$ to $n = 5$ shells is −9625.39 a.u., giving a total correlation energy of −0.1708 a.u. (including Coulomb, Gaunt, and Breit retardation). The nuclear size was again taken to be 5.75 fm for comparison with other calculations (the experimental value from Ref. [26] is 5.863 fm, which would lead to −9624.84 a.u. and −9625.01 a.u., respectively, but leaves the correlation energy unchanged). The diagonal Lagrange parameters for that calculation are listed in Table V, with the radius of maximum electronic density for each orbital. All radii are of the same order of magnitude as expected. Only 10 out of 25 orbitals have diagonal Lagrange multipliers above $-2mc^2$.

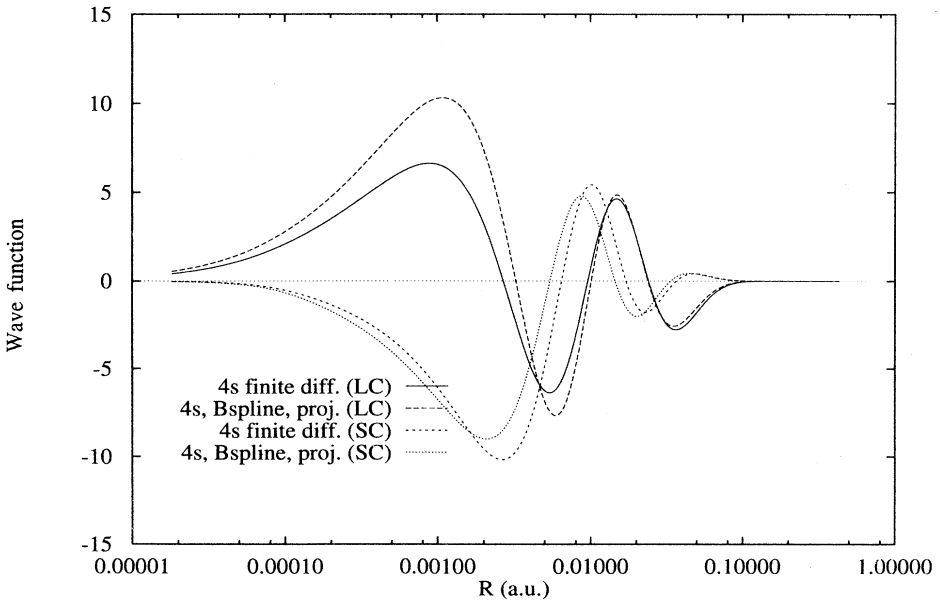

FIG. 5. Small (SC) and large (LC) components of a $4s$ orbital radial wave function (configurations $1s^2$, $2s^2$,..., $4s^2$, $Z = 92$), computed without (finite diff.) and with a projection operator. Note that the unprojected radial wave function computed with the finite-difference method or the B spline method would be indistinguishable on this plot.

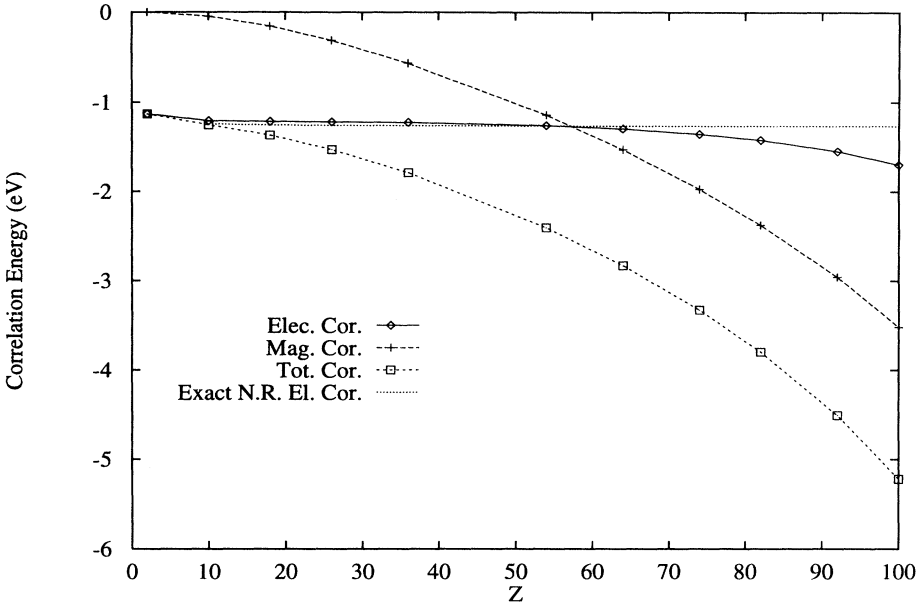

FIG. 6. Relativistic effects in the electrostatic correlation energy and the magnetic correlation energy (magnetic interaction as a first-order perturbation). The configuration set is $1s^2$, $2s^2$,..., $5g^2$. Elec. Cor., electrostatic correlation energy, Mag. Cor., magnetic correlation energy; Tot. Cor., total correlation energy. Exact N.R. El. Cor., exact nonrelativistic correlation energy from Ref. [25].

TABLE V. Examples of diagonal Lagrange parameters for Z=92. R_{max} is the radius of maximal electronic density for the orbital (a.u.).

Orbital	R_{max}	Diagonal Lagrange parameter (a.u.)
	Single configuration	
$1s$	8.13×10^{-03}	−4771.30
	$1s^2 + \cdots 5g^2$	
$1s$	8.13×10^{-03}	−4771.53
$2p_{1/2}$	9.00×10^{-03}	−11265.69
$2s$	3.48×10^{-03}	−12299.58
$2p_{3/2}$	1.03×10^{-02}	−14272.28
$3d_{3/2}$	9.47×10^{-03}	−21438.51
$3p_{1/2}$	3.72×10^{-03}	−22570.07
$3d_{5/2}$	1.03×10^{-02}	−25824.24
$3s$	1.99×10^{-03}	−26625.70
$3p_{3/2}$	4.96×10^{-03}	−30106.57
$4f_{5/2}$	9.85×10^{-03}	−32110.41
$-2mc^2$		−37555.77
$4d_{3/2}$	4.92×10^{-03}	−38114.85
$4f_{7/2}$	1.02×10^{-02}	−38398.55
$4p_{1/2}$	2.12×10^{-03}	−39360.16
$5g_{7/2}$	1.01×10^{-02}	−43315.68
$4d_{5/2}$	5.61×10^{-03}	−45838.86
$4s$	1.29×10^{-03}	−46322.78
$4p_{3/2}$	3.05×10^{-03}	−50745.68
$5f_{5/2}$	5.69×10^{-03}	−51182.19
$5g_{9/2}$	1.02×10^{-02}	−51176.68
$5d_{3/2}$	3.21×10^{-03}	−57843.99
$5p_{1/2}$	1.42×10^{-03}	−59578.14
$5f_{7/2}$	6.06×10^{-03}	−60062.99
$5d_{5/2}$	3.75×10^{-03}	−67965.32
$5s$	9.26×10^{-04}	−68639.52
$5p_{3/2}$	2.13×10^{-03}	−73224.75

In Fig. 7, I have plotted the electrostatic and magnetic correlation energies calculated with both interactions satisfying self-consistency. There is an ambiguity in the definition of correlation in that case. The reference $1s^2$ level energy changes when including the Gaunt interaction in the SCF. Still it remains an independent-particle approximation result. So if correlation is defined with reference to the Coulomb-only energy, some contributions that are not correlation will be included in the "correlation" energy. My results will thus refer to the Coulomb-Gaunt energy, except when comparing them with results from other calculations.

There are some striking features in these results, the most obvious one being the change of sign of the electrostatic correlation at high Z. This is not a sign of some problem in the calculation (the correlation energy calculated by variational means should be always negative) as the total correlation energy, which is now the only meaningful term, is still negative. What is called electrostatic correlation energy is now in fact the sum of the electrostatic correlation energy and some cross magnetic and Coulomb contributions since now the wave function contains some magnetic contributions. The different kinds of contributions are shown in Fig. 8. The MCDF method enables a summation of the series of diagrams with parallel photon lines (the ladder approximation). In those diagrams the electron lines represent bound electrons in the field from the nucleus only. Single configuration Dirac-Fock calculations sum the type-B diagrams of Fig. 8 to all orders, but taking in account only the monopole part of the interaction. When going to larger CSF sets, one does a summation of more and more multipole components of the interaction. When the Gaunt interaction is not included in the SCF, only the diagrams of type A

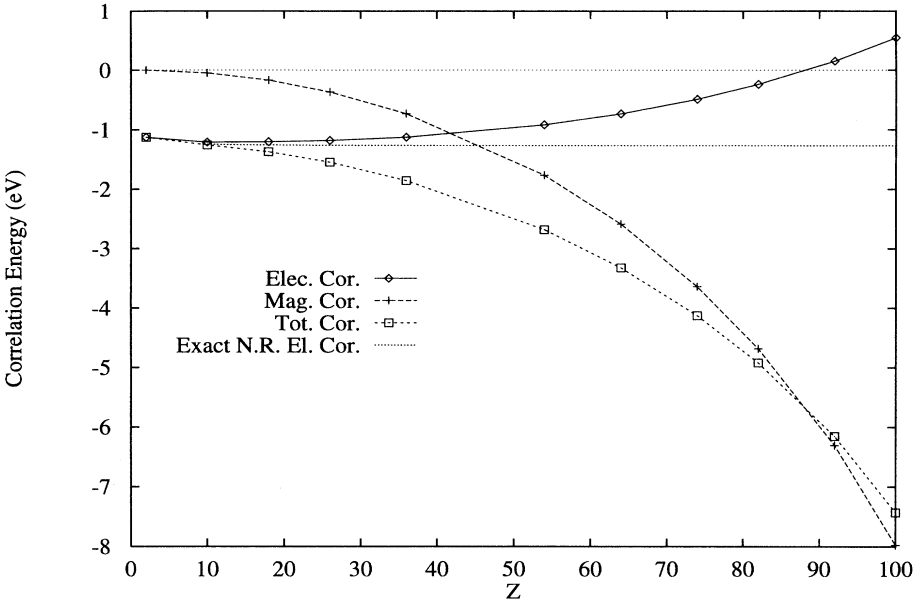

FIG. 7. Electrostatic and magnetic correlation energy (the magnetic interaction is self-consistent). The configuration set is $1s^2$, $2s^2$,..., $5g^2$. The legend is the same as in Fig. 6.

are included (one transverse photon and one or more longitudinal ones). Diagrams with at least two transverse photons are included only if the Gaunt interaction is included in the SCF. But they appear in both the Coulomb contribution to the energy (through the wave functions) and in the Gaunt contribution (through both the wave functions and the operator). This is why individual contributions to the total correlation energy lose their meaning, which leads to the strange behavior of the Coulomb contribution (which is still called Coulomb only for convenience and because in the calculation it comes from Coulomb-type integrals).

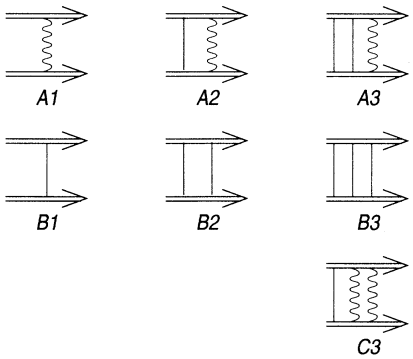

FIG. 8. Contribution to the electrostatic and the magnetic correlation energy. Double arrows represent *bound* electrons. Diagrams of type $A1$ contribute to the uncorrelated magnetic energy. Diagrams of type $A2$ and $A3$ are successive contributions to magnetic correlation when only the Coulomb potential is included in the SCF process. Diagrams of type $B2$, $B3$, etc., are contributions to the electrostatic correlation energy. Diagrams of type $C3$ are computed only when both Coulomb and Gaunt operators are included in the SCF process.

C. Discussion

The present results can be compared to other recent relativistic calculations. The first one computes exactly the second-order diagrams derived from bound-state QED [27]. The second one is an all-order relativistic many-body perturbation theory [28] and should give results very similar to the MCDF method. In both cases the no-pair approximation is used, part of the retardation is included, and diagrams of order greater than two are included. A sample of MCDF results for atomic numbers used in these two references and with identical nuclear radii [29] are presented in Table VI. In Fig. 9, I have plotted the correlation energy from all three calculations from which the nonrelativistic correlation energy has been subtracted. This thus shows the relativistic and QED contributions from these calculations. The first-order energy for getting the total energy from Ref. [27] was obtained using the Dirac-Fock program with frozen hydrogenlike orbitals. In order to get a consistent comparison with the correlation energy from Ref. [25], the reference uncorrelated energy was chosen to be the Dirac-Fock energy with only the Coulomb interaction in the SCF. Care must be taken to do the reduced mass correction to the data from Refs. [27,28], in order to compare them to the present results.

The curves in Fig. 9 can be best fitted by third-degree polynomials. This is consistent with $1/Z$ expansion theory [30], which predicts that the relativistic binding energy can be expanded as a sum of terms of the form $Z^2(Z\alpha)^{2n}/Z^p$, $n \geq 0$, $p \geq 0$ (in a.u.). The terms with $n = 0$ are all contained in the nonrelativistic correlation energy and those with $p = 0$ are contained in the hydrogenic Dirac energy. The MCDF relativistic correlation energy contribution is given by $\Delta E_{\mathrm{MCDF}} = (0.148\,86 - 0.017\,334Z + 1.9318 \times 10^{-4}Z^2 -$

TABLE VI. Results for selected cases (eV). The following abbreviations are used: Coulomb, $1s^2$ Coulomb energy (Coulomb + magnetic self-consistent). Mag, $1s^2$ magnetic energy (Coulomb + magnetic self-consistent). MP, mass polarization from Ref. [33]; NRCE, exact nonrelativistic correlation energy from Ref. [25]; RECE, relativistic contribution to electrostatic correlation energy; Mag. Corr., magnetic correlation energy; Ret. Corr., retardation correlation energy (order ω^2); Tot., total level energy, Ion., Ionization energy.

Z	Coulomb	Mag.	MP	NRCE	RECE	Mag. Corr.	Ret. Corr.	Tot.	Ion.
10	-2557.332	0.329	0.001	-1.243	0.004	-0.048	0.012	-2558.277	-1195.929
20	-10603.202	2.779	0.001	-1.257	0.022	-0.211	0.052	-10601.816	-5130.333
30	-24274.154	9.603	0.001	-1.261	0.062	-0.496	0.122	-24266.123	-11870.873
40	-43806.473	23.206	0.001	-1.263	0.135	-0.916	0.224	-43785.086	-21532.055
50	-69560.432	46.241	0.001	-1.264	0.249	-1.489	0.361	-69516.332	-34289.866
60	-102056.486	81.751	0.001	-1.265	0.412	-2.236	0.540	-101977.284	-50399.569
70	-142032.974	133.380	0.001	-1.266	0.633	-3.190	0.767	-141902.649	-70224.090
80	-190546.041	205.715	0.001	-1.266	0.923	-4.402	1.056	-190344.016	-94283.193
90	-249132.783	304.828	0.001	-1.267	1.297	-5.953	1.426	-248832.451	-123333.726
100	-320114.771	439.291	0.001	-1.267	1.775	-7.975	1.908	-319681.039	-158518.806

$5.256 \times 10^{-6} Z^3$) eV. For the all-order RMBPT calculation I obtain $\Delta E_{\rm all} = (0.148\,22 - 0.017\,472Z + 1.5844 \times 10^{-4}Z^2 - 5.280 \times 10^{-6}Z^3)$ eV. The second-order RMBPT calculation gives $\Delta E_{\rm 2nd} = (0.127\,58 - 0.018\,194Z + 1.8029 \times 10^{-4}Z^2 - 5.537 \times 10^{-6}Z^3)$ eV.

The all-order RMBPT calculation and the MCDF calculation have very close values for the coefficients of Z^0 and Z^1, while they differ in the Z^2 value. One can interpret those differences by noticing that both RMBPT calculations include the Breit retardation of Eq. (20) to second order only. In our calculation both the Gaunt interaction (19) and the Breit retardation (20) are included to all orders. The second-order RMBPT calculation, in contrast, has different values for all four coefficients, showing the effects of three and more photon exchange. The all-order and the second-order RMBPT calculations are very close (0.13 eV at $Z = 100$), showing that the higher-order Coulomb photon exchange is very small indeed. The difference between the MCDF value and the all-order RMBPT calculation shows that higher-order terms in the Breit approximation play a larger role. Both effects, however, are a small fraction of the contribution of the QED correction (higher-order retardation, virtual-pair correction, and box diagram).

Finally, to give a more precise meaning to the discussion of the preceding paragraph, I have evaluated the error in the MCDF results due to the truncation of the configuration space to $n \leq 5$. The contributions to the correlation energy of different angular quantum number l have been plotted. For each l this contribution is very well represented by a $a(l)n^{-k(l)}$ law, with $k \approx 5$. Each contribution has thus been fitted to extrapolate to infinity. Contributions from values of $l > 4$ have been deduced by extrapolating the behavior of $a(l)$ and $k(l)$. Those extrapolations have been done for both the nonrelativistic MCHF correlation energy and the MCDF correlation en-

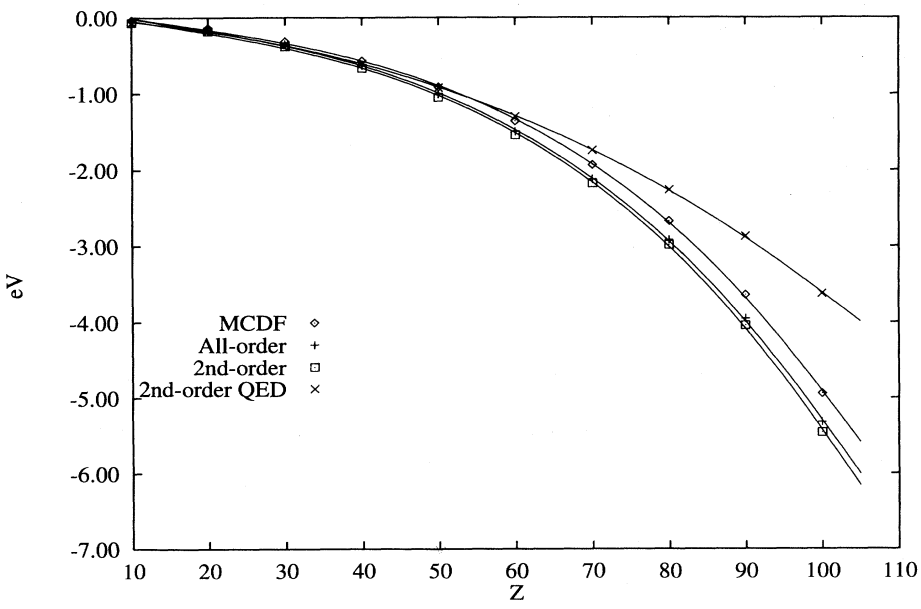

FIG. 9. Comparison of total correlation energies. MCDF, this work, all-order RMBPT, Ref. [28]; second-order RMBPT, Ref. [27]; exact second order, complete second-order QED calculation from Ref. [27]. Solid lines represents the fits given in the text.

ergy at $Z = 10$ and $Z = 100$. The differences between extrapolated MCHF values and the MCHF results are -0.021 eV ($Z = 10$) and -0.023 eV ($Z = 100$), while the differences between the exact nonrelativistic and the MCHF values are -0.032 eV and -0.038 eV, respectively. The differences between the MCDF extrapolated values and the MCDF values are, respectively, -0.012 eV and -0.136 eV. So most of the effect of the truncation of the configuration space is taken into account by using the exact nonrelativistic correlation energy in place of the MCHF value for low Z, while a sizable error comes from the evaluation of relativistic correction at high Z. The final correction on the MCDF value can then be estimated to -0.001 eV at $Z = 10$ and -0.113 eV at $Z = 100$. The extrapolated MCDF value for $Z = 100$ can be deduced from the above discussion and is $\Delta E_{\mathrm{MCDF}} = -6.321$ eV. The all-order value is $\Delta E_{\mathrm{all}} = -6.588$ eV, the second-order RMBPT value is $\Delta E_{\mathrm{2nd}} = -6.725$ eV, and the exact second-order QED contribution is -4.890 eV. From this I conclude that at $Z = 100$ the effect of second-order QED corrections is $+1.835$ eV, which is larger than the sum of higher-order relativistic Coulomb corrections ($+0.137$ eV) and higher-order magnetic and (Breit) retardation corrections ($+0.267$ eV). Finally, I have evaluated the effect of higher-order retardation from Eq. (21) and found $+0.296$ eV. The second-order part of this contribution is already included in the QED correction from Ref. [27] and should not be included simultaneously.

I want to stress again that those values are for a reference state with only the Coulomb interaction included in the SCF, while the correlation contributions in Table VI are calculated for a reference state with the Gaunt interaction in the SCF. Obviously this is just a matter of convention and leads to the same total level energy.

CONCLUSION

In this paper an alternative method for computing correlation contribution using the MCDF approximation has been described. In the process of exploring the properties of this method, it has been found that one needs to include proper projection operators onto states with $E > -2mc^2$ to get meaningful results at high Z. This is in complete agreement with what has been advocated for years by Sucher [3] and Mittleman [2]. I have shown that the inclusion of these projection operators leads to numerically significant effects and enables one to compute higher-order corrections, which up to now could be obtained only by relativistic many-body perturbation theory. A complete calculation of the lower level in two-electron ions using this method is in progress and will be published separately. I have been able to compare our results for $Z = 100$ with second-order and all-order RMBPT and second-order QED calculation and I have shown that all-order Gaunt and Breit effects are larger than all-order Coulomb effects at high Z. Both effects are relatively small compared to QED corrections ($\approx 30\%$), but larger than what had been estimated from extrapolation of the low Z leading three-photon exchange contribution [31,32]. For practical purposes, the best theoretical value can be obtained by combining the present MCDF calculation with the ΔE_{QED} from Ref. [27]. This will lead to a result exact to second order and including all Coulomb, magnetic, and retardation corrections from three and more photon exchange in the ladder approximation. If the ratio between the non-QED part and the QED part of those higher-order diagrams is of the same order as in the second-order diagrams (a likely hypothesis), higher-order QED correction should be completely negligible. The nonradiative part of the ground-state energy in two-electron heavy ions can thus be considered to be as precise as the one-electron energy. Computing the two-electron self-energy and higher-order radiative corrections to the same accuracy, however, is going to require a major effort, which has been undertaken by many workers.

ACKNOWLEDGMENTS

I first want to express my gratitude to Dr. J. P. Desclaux. I could not have undertaken this work without his encouragement and his help to graft the method described in this paper to his MCDF code. We had also many fundamental discussions about the physics involved. I wish to thank Dr. A. M. Mårtenson-Pendrill and Dr. E. Lindroth for communicating unpublished results and for very enlightening discussions on their work. I wish also to thank Dr. Y.-K. Kim for many helpful comments on the manuscript and for support for several stays at NIST, during which I worked on this project. Several exchanges with Professor C. Froese-Fischer helped me clarify a number of issues in the interpretation of the results. I had a very interesting discussion with Dr. P. J. Mohr and Professor W. R. Johnson about higher-order corrections, which helped me revise the discussion and conclusion of this work. Finally, I thank Professor J. P. Briand for his interest in this work.

[1] G. E. Brown and D. E. Ravenhall, Proc. R. Soc. London Ser. A **208**, 552 (1951).
[2] M. H. Mittleman, Phys. Rev. A **24**, 1167 (1981).
[3] J. Sucher, Phys. Rev. A **22**, 348 (1980).
[4] J. Sucher, in *Foundations of the Relativistic Theory of Many-Electron Atoms*, edited by G. Mailli (Plenum, New York, 1982).
[5] I. P. Grant, Adv. Phys. **19**, 747 (1970).
[6] J. P. Desclaux, Comput. Phys. Commun. **9**, 31 (1975).
[7] W. R. Johnson and J. Sapirstein, Phys. Rev. Lett. **57**, 1126 (1986).
[8] W. R. Johnson, S. Blundell, and J. Sapirstein, Phys. Rev. A **37**, 2764 (1988).
[9] S. A. Blundell, W. R. Johnson, and J. Sapirstein, Phys. Rev. A **38**, 4961 (1989).
[10] S. A. Blundell, W. R. Johnson, Z. W. Liu, and J. Sapirstein, Phys. Rev. A **40**, 2233 (1989).
[11] S. A. Blundell, W. R. Johnson, Z. W. Liu, and J.

Sapirstein, Phys. Rev. A **39**, 3768 (1989).
[12] J. L. Heully, I. Lindgren, E. Lindroth, and A. M. Mårtensson-Pendrill, Phys. Rev. A **33**, 4426 (1986).
[13] E. Lindroth, Phys. Rev. A **37**, 316 (1988).
[14] S. Salomonson and P. Öster, Phys. Rev. A **40**, 5548 (1989).
[15] A. A. Broyles, Phys. Rev. A **39**, 4939 (1989).
[16] A. A. Broyles, Phys. Rev. A **38**, 1137 (1988).
[17] G. Hardekopf and J. Sucher, Phys. Rev. A **30**, 703 (1984).
[18] I. P. Grant and H. M. Quiney, Adv. At. Mol. Phys. **23**, 37 (1988).
[19] O. Gorceix, P. Indelicato, and J. P. Desclaux, J. Phys. B **20**, 639 (1987).
[20] P. Indelicato and J. P. Desclaux, Phys. Rev. A **42**, 5139 (1990).
[21] P. Indelicato and J. P. Desclaux, Phys. Scr. **T46**, 110 (1993).
[22] W. H. Press, B. P. Flannery, S. A. Teukolsky, and W. T. Vetterling, *Numerical Recipes* (Cambridge University Press, Cambridge, 1986).
[23] D. C. Griffin, R. D. Cowan, and K. L. Andrew, Phys. Rev. A **3**, 1233 (1971).
[24] S. Salomonson and P. Öster, Phys. Rev. A **40**, 5559 (1989).
[25] P. Blanchard, Phys. Rev. A **13**, 1698 (1976).
[26] J. Zumbro, E. B. Shera, Y. Tanaka, J. C. E. Bemis, R. A. Naumann, M. V. Hoehn, W. Reuter, and R. M. Steffen, Phys. Rev. Lett. **53**, 1888 (1984).
[27] S. A. Blundell, P. J. Mohr, W. R. Johnson, and J. Sapirstein, Phys. Rev. A **48**, 2615 (1993).
[28] D. R. Plante, W. R. Johnson, and J. Sapirstein, Phys. Rev. A **49**, 3519 (1994).
[29] W. R. Johnson and G. Soff, At. Data Nucl. Data Tables **33**, 405 (1985).
[30] H. T. Doyle, Adv. At. Mol. Phys. **5**, 377 (1969).
[31] P. J. Mohr (private communication).
[32] P. J. Mohr, Nucl. Instrum. Methods B **87**, 232 (1994).
[33] G. W. F. Drake, Can. J. Phys. **66**, 586 (1988).